Prepared for submission to JINST

Instrumentation for Colliding Beam Physics (INSTR-20)
24–28 February 2020
Budker Institute of Nuclear Physics (BINP), Novosibirsk, Russia

A High-Granularity Timing Detector for the Phase-II upgrade of the ATLAS Calorimeter system: detector concept, description, R&D and beam test results

L. Castillo García,[a,1] **on behalf of the ATLAS HGTD Collaboration**

[a] *Institut de Física d'Altes Energies (IFAE), The Barcelona Institute of Science and Technology (BIST), Carrer Can Magrans s/n, Edifici Cn, UAB campus, E-08193 Bellaterra (Barcelona), Spain*

E-mail: lucia.castillo.garcia@cern.ch

Abstract: The increase of the number of interactions at the High Luminosity LHC will have a severe impact on the ATLAS detector reconstruction and trigger performance. The end-cap and forward regions, where the Liquid Argon calorimeter has coarser granularity and the inner tracker has poorer momentum resolution, will be particularly affected. A High Granularity Timing Detector (HGTD) is proposed in front of the Liquid Argon end-cap calorimeters for pile-up mitigation and for luminosity measurement. It will cover the pseudo-rapidity range $2.4 < |\eta| < 4.0$. Two silicon sensors double-sided layers on each end-cap will provide precision timing information for minimum ionising particles in order to assign each particle to the correct vertex. Readout cells have a size of $1.3\,\text{mm} \times 1.3\,\text{mm}$, leading to a highly granular detector with over 3.6 million channels. The Low Gain Avalanche Detectors (LGAD) technology has been chosen for the HGTD detector as it provides a compact sensor with large signal over noise ratio leading to excellent timing performance. The requirements and overall specifications of the HGTD will be presented. LGAD R&D campaigns were carried out to study the sensors and their radiation hardness. Latest laboratory and test beam results will be presented.

Keywords: LGAD, Silicon sensors, Timing detectors, HL-LHC, ATLAS, HGTD

ATL-LARG-PROC-2020-007
13 May 2020

[1] Corresponding author.

Contents

1 Introduction

The Large Hadron Collider (LHC) [1] is currently in shutdown for maintenance and LHC experiments are being upgraded to be ready to take data in 2021 for a period of 4 years (Run 3). A second upgrade phase is foreseen in 2025 for the High-Luminosity LHC (HL-LHC) [2, 3] where faster and more radiation hard detectors are needed to cope with higher track multiplicity and higher radiation levels. With a luminosity of 7.5×10^{34} cm^{-2}s^{-1} the average number of interactions per bunch-crossing (pile-up) at HL-LHC will be about 200, resulting in 1.8 vertices/mm on average. In this high pile-up environment it will be very challenging to efficiently assign charged particles to the correct production vertices. The increased particle flux will degrade the vertex reconstruction and the physics objects performance in the ATLAS experiment [4] in the forward region, where, compared to the central region, the Liquid Argon (LAr) [5] electromagnetic calorimeter has coarser granularity and the inner tracker poorer momentum and position resolution. In this context, timing information can be used to resolve the ambiguities. In a high pile-up event, multiple vertices will occur in the same z but, by adding timing information, vertices could be distinguished. Thus the High Granularity Timing Detector (HGTD) [6] is proposed to mitigate pile-up effects and improve the overall ATLAS performance in the forward region by combining the HGTD high-precision time measurement with the Inner Tracker (ITk) [7, 8] position information.

2 High Granularity Timing Detector (HGTD)

2.1 Detector overview and requirements

The HGTD is designed to operate with a pile-up of ~ 200 and for the entire HL-LHC running period. However, to ensure the desired performance part of the detector will have to be replaced (see Sec. 2.4). The detector will be installed in front of the LAr end-cap calorimeters in ATLAS where the space available is limited. Consequently, a silicon based detector technology is chosen. The HGTD detector consists of two double-sided layers mounted on two cooling disks per end-cap. Table 1 summarizes the main requirements. HGTD will cover the pseudo-rapidity range $2.4 < |\eta| < 4.0$. Segmented sensors will be used with a pad size of $1.3 \times 1.3\,\text{mm}^2$ that is expected to provide a maximum occupancy below 10% for a radius below 230 mm, small dead areas between the pads and low sensor capacitance. The sensors will be operated at $-30\,^{\circ}\text{C}$ to mitigate the impact of irradiation. The ASIC needs to meet the timing and radiation hardness requirements, and will provide the functionality to count the number of hits registered in the sensors in order to perform bunch-by-bunch luminosity measurements. To ensure the correct performance of the ASIC, the collected charge per hit should be bigger than 4 fC. The hit detection efficiency should be higher than 95%. A time resolution of 35 ps per hit is required at the start of HL-LHC (Run 4) and 70 ps per hit at the end of HL-LHC running period.

Table 1. Main parameters of the HGTD.

Pseudo-rapidity coverage	$2.4 < \|\eta\| < 4.0$
Thickness in z	75 mm (+50 mm moderator)
Position of active layers in z	$z \approx \pm 3.5$ m
Weight per end-cap	350 kg
Radial extension:	
Total	110 mm $< r <$ 1000 mm
Active area	120 mm $< r <$ 640 mm
Pad size	$1.3\,\text{mm} \times 1.3\,\text{mm}$
Active sensor thickness	50 µm
Number of channels	3.6 M
Active area	$6.4\,\text{m}^2$
Module size	30 x 15 pads ($4\,\text{cm} \times 2\,\text{cm}$)
Modules	8032
Collected charge per hit	> 4.0 fC
Hit detection efficiency	> 95%
Average time resolution per hit (start and end of operational lifetime)	
$2.4 < \|\eta\| < 4.0$	≈ 35 ps (start), ≈ 70 ps (end)
Average time resolution per track (start and end of operational lifetime)	≈ 30 ps (start), ≈ 50 ps (end)

2.2 Detector layout

Each detector layer consists of three rings covering different pseudo-rapidity ranges as shown in Figure 1 (left). The HGTD modules are mounted on the cooling disks in such a way that they partially overlap between layer sides optimising the uniformity in performance as a function of radius. In the inner ring (120 mm $< r <$ 230 mm) an overlap of 70% results in 2.6 hits per track on

average, in the middle ring (230 mm $< r <$ 470 mm) an overlap of 54% results in 2.4 hits per track on average and in the outer ring (470 mm $< r <$ 660 mm) an overlap of 20% results in 2.0 hits per track on average. Each cooling disk is physically separated in two half circular disks and layers are rotated 15° to 20° in opposite direction to avoid gaps.

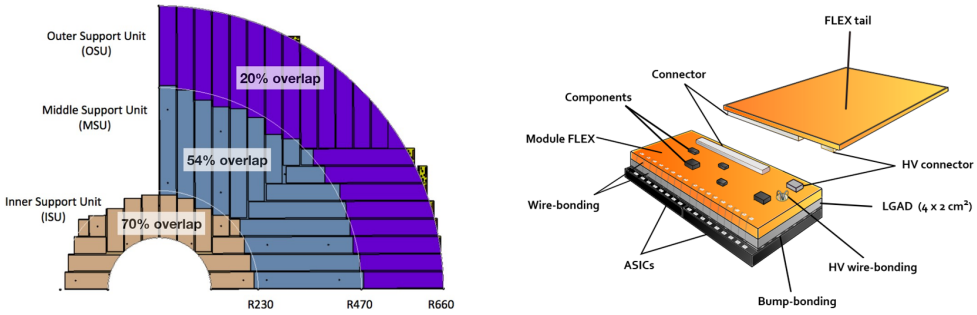

Figure 1. View of the modules inserted on the inner, middle and outer ring half disk support units (left). View of an HGTD hybrid module equipped with its read-out flex cable tail (right).

2.3 Hybrid module

The HGTD modules are hybrids made of an LGAD sensor [9] connected through bump bonding to a custom ASIC, named ATLAS LGAD Time Read Out Chip (ALTIROC). The total number of modules to be installed in the detector is 8032. The ALTIROC ASIC should have low noise and low power consumption (<100 mW/cm^2). It provides the Time Of Arrival (TOA) and the Time Over Threshold (TOT) measurements of the traversing particle. The ASIC contribution to the time resolution should be smaller than 25 ps. Its discriminator threshold is about 2 fC. The chip is being developed in different phases: a first iteration, ALTIROC0 [10, 11], in a 2×2 array incorporating the single-pixel analog readout (preamplifier and discriminator); a second iteration, ALTIROC1, in a 5×5 array with the full single-pixel readout (analog + digital) and a final version in a 15×15 array of total size of 20×22 mm^2.

The LGAD is a n-on-p silicon planar detector with a highly doped multiplication layer that amplifies the signal. It achieves 30 ps time resolution before irradiation and the final sensor will have 15×30 pads for a total area of 4×2 cm^2. The HGTD hybrid modules will include two ASICs per sensor. A view of a module is shown in Figure 1 (right). The sensor is glued to a small flex cable and the signal lines of the ASIC are wire bonded to it as well. The bias voltage for the sensor is provided to the back-side through a hole in the flex. A second long flex cable routes all connections between the ASIC and the peripheral on-detector electronics.

2.4 Radiation hardness

The detector will have to cope with very high radiation levels. For the inner radius, at the end of HL-LHC (4000 fb^{-1}), the maximum fluence will be $2.5{\times}10^{15}$ n_{eq}/cm^2 and the Total Ionising Dose (TID) will be 2 MGy. These values take into account a replacement of about 52% of the total amount of modules, the innermost ring will be replaced three times (after each 1000 fb^{-1}) and the

middle ring just once (at half lifetime, 2000 fb^{-1}). The values also account for uncertainties in the simulation and low dose rate effects on the electronics with a safety factor of 1.5 for sensors and 2.25 for electronics, since they are more sensitive to the TID. Figure 2 shows the fluence levels from Fluka simulations [12] as a function of radius for the different particles. In the inner ring the contribution of neutrons and charged particles is similar whereas in the middle and outer rings the dominant contribution comes from neutrons.

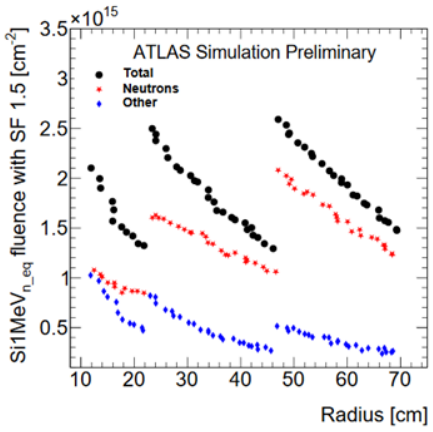

Figure 2. Expected Si1MeV$_{n_{eq}}$ radiation levels in HGTD, using Fluka simulations, as a function of the radius considering a replacement of the inner ring every 1000 fb^{-1} and the middle ring replaced at 2000 fb^{-1} [13]. Modified from [14] taking into account the replacement strategy.

3 LGAD R&D program

An extensive R&D program on the sensor LGAD technology is ongoing in close collaboration with RD50 [15] and manufacturers as Centro Nacional de Microelectrónica (CNM, Barcelona), Hamamatsu Photonics (HPK, Japan), Fondazione Bruno Kessler (FBK, Italy) and Novel Device Laboratory (NDL, China). The performance of LGAD sensors produced by the four vendors is being investigated in laboratories and in charged-particle beams. In order to determine if they can provide the required time resolution in the harsh radiation environments, different LGAD geometries and doping materials have been evaluated at different irradiation levels. Throughout this R&D program, several irradiation campaigns have been taken place at various facilities with different particle types and energies that are representative for the ones expected in HGTD [6] operations: JSI Ljubljana (1 MeV n), CYRIC (70 MeV protons), Los Alamos (800 MeV protons), CERN PS (23 GeV protons) and PSI (192 MeV pions).

3.1 Laboratory measurements

A ^{90}Sr source is used in the laboratory to characterize the LGAD response to minimum ionising particles (2 MeV electrons). Figure 3 (left) illustrates the set-up. The source container is mounted on a 3D printed support together with an aluminium L-shaped support frame. LGAD sensors are assembled on custom readout boards [16] mounted back to back on an aluminium L-shaped support

frame and aligned with respect to the source beam axis. This system is operated inside a climate chamber at low temperatures (down to −30 °C). Dry air is provided to avoid condensation on the sensor surface which could damage the sensor. A non-irradiated LGAD, previously calibrated and with a known performance, is used as time reference. The output analog signal from the readout board is recorded with an oscilloscope for different bias voltages. Data is saved for off-line waveform processing. For each event, the charge from the recorded waveform is calculated as the integral of the signal area. A charge distribution is plotted and fitted using a Landau-Gauss convoluted function where the collected charge is defined as the most probable value of the fitted function. Figure 3 (right) shows the collected charge as a function of the bias voltage for HPK sensors [17] irradiated at different fluences up to 6×10^{15} n_{eq}/cm^2 [18]. These sensors meet the HGTD requirement of collecting at least 4 fC for an efficient HGTD operation up to the end of HL-LHC phase.

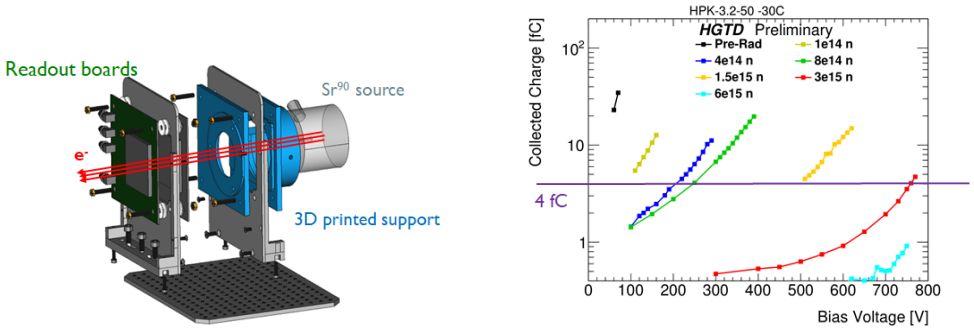

Figure 3. Sketch of timing set-up in the laboratory (left). Collected charge as a function of the bias voltage for HPK type-3.2 LGADs irradiated at different fluences (right) [13].

3.2 Test beam campaigns

Un-irradiated and irradiated LGADs and first HGTD modules (with the ALTIROC0) have been characterized in charged-particle beams [11, 19]. Tests have been conducted at the H6A-B beam line at the CERN SPS facility [20] with 120 GeV pions and at TB22 beam line at the DESY facility [21] with 5 GeV electrons. In the following sections, more recent results obtained at DESY for a 1×1 mm^2 CNM Gallium-doped LGAD irradiated to 3×10^{15} n_{eq}/cm^2 are presented.

3.2.1 Experimental setup

A pixel EUDET-type telescope [22], DURANTA, was used to provide particle track information. In addition, a reference tracking plane, using the FE-I4 [23] readout chip, was also used for sensor alignment and triggering purposes by defining a region of interest that contained the projected area of the different LGADs. This implementation of a region of interest resulted in a reduced hit rate. Upstream and downstream scintillators in the DURANTA telescope, HitOR signal from the FE-I4 and oscilloscope auxilliary output are integrated in the trigger system which was handled by the EUDET Trigger Logic Unit (TLU) [24] to synchronize the telescope with the HGTD DAQ system. Since at DESY the beam is continuous, the use of a busy signal implemented with standard NIM electronics was essential to allow the oscilloscope to empty the buffer and be ready to restart taking

data. LGAD sensors were installed in a light-tight cooling box mounted on a remote controlled stage[1] that was placed between the two telescope arms. In this way, the sensors were aligned with respect to the beam axis. Dry ice was used to keep irradiated sensors cold. The temperature was continuously monitored and dry ice refilled to keep sensors below −20 °C. Data taking runs correspond to different bias voltages studied.

3.2.2 Data analysis and results

Data taken at the test beams have been analyzed using two software frameworks. Native data from the telescope containing the track information was reconstructed with the EUTelescope software [25, 26] v01-19-02 using the General Broken Lines (GBL) algorithm to take into account the multiple scattering of 5 GeV electrons. Binary data from the oscilloscope was analyzed using a C++ based software, LGADUtils [27], which performs the data conversion, the waveform processing with a calculation of the signal properties and merges the oscilloscope and telescope data into a single ROOT ntuple.

As it is explained in Sec. 3.1, the collected charge for each run is calculated. Figure 4 (left) shows the collected charge as a function of the bias voltage for a CNM Gallium-doped LGAD. After irradiation to 3×10^{15} n_{eq}/cm^2 this sensor reaches the 4 fC requirement for an optimal ALTIROC performance, and in particular 5.3 fC at 740 V.

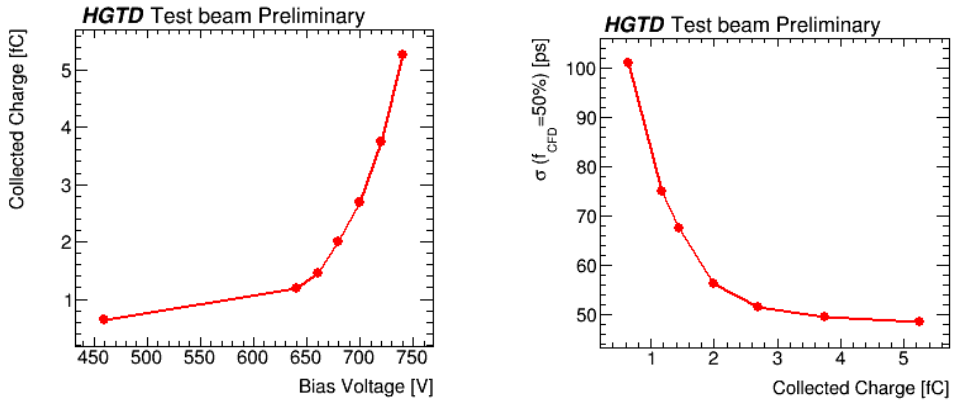

Figure 4. Collected charge as a function of the bias voltage (left) and time resolution as a function of the collected charge (right) for a CNM Gallium-doped LGAD irradiated to 3×10^{15} n_{eq}/cm^2 [13].

Similarly to the collected charge procedure, for each event in a run, the TOA of the recorded waveform is calculated as the time crossing a given threshold using the Constant Fraction Discriminator (CFD) method. The threshold corresponds to a certain fraction of the the signal amplitude. This CFD fraction is defined by the dominant contribution to the time resolution. In the case of an un-irradiated sensor the dominant contribution is the Landau term whereas for an irradiated sensor the dominant effect is the noise, therefore a higher threshold is required. In order to perform timing measurements a start time is required. The time reference signal was provided by a non-irradiated

[1]Stage system from Physik Instrumente (PI).

LGAD. A time difference distribution was made between the time at a CFD=50% for the CNM Gallium sensor and the time at a CFD=20% for the reference sensor. The time resolution was found to be 48.7 ps at 740 V. The contribution of the reference sensor of 29.7 ps is already subtracted. This sensor meets the HGTD timing requirement of 70 ps at the end of HL-LHC. Figure 4 (right) shows the time resolution at a CFD fraction of 50% as a function of the collected charge.

Figure 5 (left) displays the mask of the $1 \times 1\,\text{mm}^2$ CNM S-type LGAD prototype sensor, where the area of the gain layer implantation is $0.7 \times 0.7\,\text{mm}^2$. Figure 5 (right) shows the efficiency as a function of the reconstructed position of particles at 740 V. The efficiency is defined as the ratio between the number of tracks with a collected charge larger than 2 fC and the total number of reconstructed tracks that are extrapolated to the sensitive area of the sensor, where only single track events are considered. A cut at 2 fC, equivalent to 15 mV, is applied because it is the minimum charge required by the ALTIROC discriminator. Each bin size of this 2D map is $50{\times}50\,\mu\text{m}^2$. After 3×10^{15} n_{eq}/cm^2, this CNM LGAD is still very efficient in the centre with an average efficiency of 99.1% whereas the edges are less efficient.

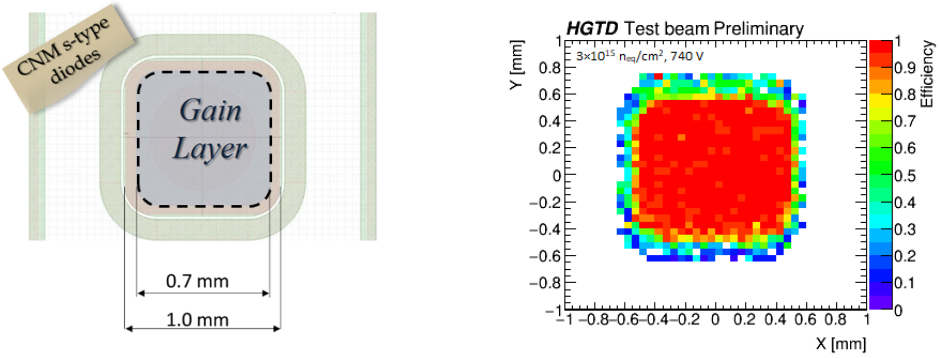

Figure 5. Mask of a CNM S-type LGAD (left). Efficiency as a function of the reconstructed position of particles for the full sensor at 740 V (right) [13].

A 2D timing map is also made in a similar way as the efficiency 2D map. Figure 6 shows the time resolution as a function of the reconstructed particle position for the full sensor (left) and for the central area (right). Each bin size is $100 \times 100\,\mu\text{m}^2$ to ensure sufficient statistics. A cut at 2 fC is also applied. As expected, time resolution degrades at the edges which also suffers from low statistics. In the central area the performance is quite homogeneous with an average time resolution of about 55 ps. The central area matches the gain layer size of $0.7 \times 0.7\,\text{mm}^2$, as it is shown in Figure 5 (left).

4 Conclusions and outlook

Performing track-to-vertex association in the HL-LHC era presents a challenge to ATLAS, especially at high η. The HGTD detector is proposed to mitigate pile-up effects and improve the reconstruction and trigger performance in the forward region. The HGTD will provide two double-sided layers of

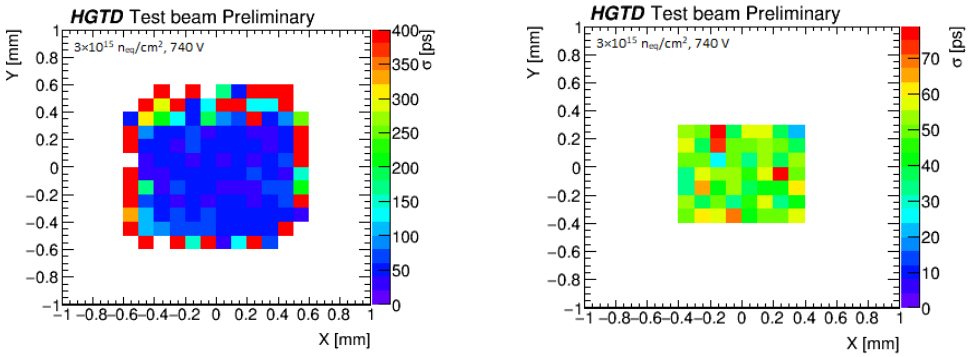

Figure 6. Time resolution as a function of the reconstructed position of particles for the full sensor (left) and for the gain layer area (right) [13].

LGAD sensors with the target of delivering a track time information better than 70 ps at the end of the HL-LHC data taking. The performance of a 1×1 mm^2 CNM Gallium-doped LGAD irradiated to 3×10^{15} n$_{eq}$/cm^2 has been presented. Parameters such as collected charge, time resolution and efficiency meet the HGTD requirements. Further analysis of other samples is ongoing. More tests in the laboratory and in charged-particle beams are foreseen this year.

Acknowledgments

This work was partially funded by MINECO, Spanish Government, under grant RTI2018-094906-B-C21. This project has received funding from the European Union's Horizon 2020 research and innovation programme under the Marie Sklodowska-Curie grant agreement No. 754510. The measurements leading to these results have been performed at the Test Beam Facility at DESY Hamburg (Germany), a member of the Helmholtz Association (HGF).

References

[1] L. Evans et al. *LHC Machine*, *JINST* **3** (2008) S08001.

[2] O. Brüning, L. Rossi, *High Luminosity Large Hadron Collider: A description for the European Strategy Preparatory Group, Tech. Rep.* **CERN-ATS-2012-236** (2012).

[3] G. Apollinari et al., *High-Luminosity Large Hadron Collider (HL-LHC): Technical Design Report V.0.1*, *CERN Yellow Reports: Monographs*, CERN, (2017) http://cds.cern.ch/record/2284929.

[4] ATLAS Collaboration, *The ATLAS Experiment at the CERN Large Hadron Collider*, *JINST* **3** S08003.

[5] M. Aleksa et al., *ATLAS Liquid Argon Calorimeter Phase-I Upgrade Technical Design Report* **CERN-LHCC-2013-017**, (2013) ATLAS-TDR-022 https://cds.cern.ch/record/1602230.

[6] ATLAS Collaboration, *Technical Proposal: A High-Granularity Timing Detector for the ATLAS Phase-II Upgrade, tech. rep.* **CERN-LHCC-2018-023**, CERN, (2018) https://cds.cern.ch/record/2623663.

[7] ATLAS Collaboration, *Technical Design Report for the ATLAS Inner Tracker Strip Detector* **CERN-LHCC-2017-005**, (2017) ATLAS-TDR-025 https://cds.cern.ch/record/2257755.

[8] ATLAS Collaboration, *Technical Design Report for the ATLAS Inner Tracker Pixel Detector* **CERN-LHCC-2017-021**, (2017) ATLAS-TDR-030 https://cds.cern.ch/record/2285585.

[9] G. Pellegrini et al., *Technology developments and first measurements of Low Gain Avalanche Detectors (LGAD) for high energy physics applications*, *Nucl. Instrum. Meth. A* **765** (2014) 12.

[10] C. De La Taille et al., *ALTIROC0, a 20 pico-second time resolution ASIC for the ATLAS High Granularity Timing Detector (HGTD)* in *Proceedings of the Topical Workshop on Electronics for Particle Physics (TWEPP-17)*, Santa Cruz, California, U.S.A, September 2017, *PoS* **TWEPP-17** (2018) 006.

[11] C. Agapopoulou et al., *Performance of a Front End prototype ASIC for picosecond precision time measurements with LGAD sensors*, (2020), arXiv:2002.06089.

[12] J. C. Armenteros, A. Cimmino, S. Roesler, H. Vincke, *FLUKA studies of dose rates in the ATLAS standard opening scenario., tech. rep.*, http://accapp17.org/wp-content/2017/data/pdfs/108-22886.pdf.

[13] *LAr HGTD Public Plots:* https://twiki.cern.ch/twiki/bin/view/AtlasPublic/LArHGTDPublicPlots.

[14] *Radiation Simulation Public Plots (HGTD results Dec 2019):* https://twiki.cern.ch/twiki/bin/view/AtlasPublic/RadiationSimulationPublicResults#HGTD_results_Dec_2019.

[15] The RD50 collaboration: https://rd50.web.cern.ch/rd50.

[16] Z. Galloway et al., *Properties of HPK UFSD after neutron irradiation up to* 6×10^{15} n_{eq}/cm^2, *Nucl. Instr. Meth. A* **940** (2019) Pages 19–29.

[17] X. Yang et al., *Layout and Performance of HPK Prototype LGAD Sensors for the High-Granularity Timing Detector*, arXiv:2003.14071.

[18] X. Shi et al., *Radiation Campaign of HPK Prototype LGAD sensors for the High-Granularity Timing Detector (HGTD)* presented at HSTD12, Hiroshima, Japan, Dec 2019, arXiv:2004.13895.

[19] C. Allaire et al., *Beam test measurements of Low Gain Avalanche Detector single pads and arrays for the ATLAS High Granularity Timing Detector*, *JINST* **13** (2018) P06017, arXiv:1804.00622.

[20] CERN SPS North Area: http://sba.web.cern.ch/sba/BeamsAndAreas/H6/H6_presentation.html.

[21] R.Diener et al., *The DESY II test beam facility*, *Nucl. Instr. Meth. A* **922** (2019) Pages 265–286.

[22] H.Jansen et al., *Performance of the EUDET-type beam telescopes*, *EPJ Techniques and Instrumentation* **3** (2016), arxiv:1603.09669v2.

[23] U. Koetz, I. Rubinskiy, *User Manual: ATLAS FE-I4A Pixel Module as a Trigger Plane for the Beam Telescope*, https://telescopes.desy.de/images/0/08/131014_koetz-rubinsky_FEI4_as_trigger_plane.pdf.

[24] D. Cussans, *Description of the JRA1 Trigger Logic Unit (TLU), v0.2c, Tech. Rep.*, (2009), http://www.eudet.org/e26/e28/e42441/e57298/EUDET-MEMO-2009-04.pdf.

[25] I. Rubinskiy, *EUTelescope. Offline track reconstruction and DUT analysis software*, Tech. Rep. EUDET-Memo-2010-12, (2010), https://www.eudet.org/e26/e28/e86887/e107460/EUDET-Memo-2010-12.pdf.

[26] *EUTelescope: A Generic Pixel Telescope Data Analysis Framework*, http://eutelescope.web.cern.ch/.

[27] *LGADUtils: A C++ based framework for waveform analysis*, https://gitlab.cern.ch/egkougko/lgadutils.